CRPP, ASSOCIATION EURATOM - CONFEDERATION SUISSE, EPFL
INTERNATIONAL SCHOOL OF PLASMA PHYSICS «PIERO CALDIROLA»

Theory of Fusion Plasmas

**PROCEEDINGS OF THE
JOINT VARENNA-LAUSANNE INTERNATIONAL WORKSHOP
HELD AT**

Villa Monastero - Varenna, Italy

24-28 August, 1992

edited by

E. Sindoni
Dipartimento di Fisica
Università di Milano
Milano, Italy

J. Vaclavik
CRPP-EPFL
Lausanne, Switzerland

Editrice Compositori   Società Italiana di Fisica

1	Zenouda, Jr.	15	G. Forgaccia	29	C.F.F. Karney	43	D. Pifferetti
2	A. Pletzer	16	D. Borba	30	M. Romé	44	G.P. Lampis
3	K. Hamamatsu	17	S.C. Guo	31	J.-D. Zenouda	45	J.B. Taylor
4	Mrs. Hamamatsu	18	F. Porcelli	32	D. Schnack	46	D. Palumbo
5	M. Bornatici	19	H.J. de Blank	33	A. Bondeson	47	A.H. Glasser
6	D. Farina	20	X. Garbet	34	H. Biglari	48	W. Horton
7	L. Villard	21	F. Romanelli	35	E. Lazzaro	49	T. Hayashi
8	W.A. Cooper	22	R. Fitzpatrick	36	T.E. Stringer	50	J. Killeen
9	A. Cardinali	23	R. Dendy	37	P.R. Thomas	51	A. Sanguanini
10	Zenouda, Jr.	24	E.K. Maschke	38	M. Terrier	52	S. Sanguanini
11	Mrs. Zenouda	25	L. Chen	39	J. Nuehrenberg	53	S. Sen
12	Z. Yoshida	26	F. Zonca	40	J. Vaclavik	54	R. Mett
13	G. Cicconi	27	R.D. Parker	41	B. Scott	55	E. Sindoni
14	R. Pozzoli	28	R.G. Storer	42	P. Halter		

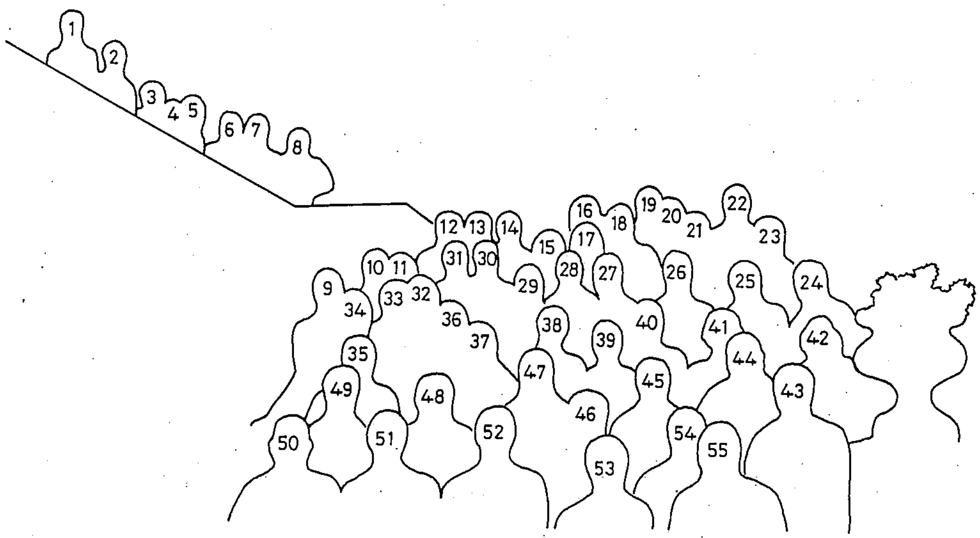

Technical Editing by Carmen Vasini

Published for the
Società Italiana di Fisica
Via L. degli Andalò 2 - 40124 BOLOGNA - Italy

by

Editrice Compositori
Via Stalingrado 97/2 - 40128 BOLOGNA - Italy

ISBN 88-7794-049-2

ISPP-12 «Piero Caldirola»
Theory of Fusion Plasmas
E. Sindoni and J. Vaclavik (Eds.)
SIF, Bologna 1992

NUMERICAL SIMULATIONS OF TURBULENCE-PROBLEM OF SELF-ORGANIZATION

W. Horton, D. Lindberg, X. Su, J. Liu, and P.J. Morrison
Institute for Fusion Studies
The University of Texas at Austin
Austin, Texas 78712

Abstract

Once sufficient energy is invested in the fields of plasma waves or hydrodynamic flows, the nonlinearity of the system plays a dominant role competing with dispersion and dissipation to form coherent self-organized structures. The nonlinear drift wave equations describe the growth of turbulent fluctuations and the formation of coherent vortices. The existence of the vortices even in the presence of the driving mechanism and magnetic shear is especially clear in the case of ∇T_i-drift modes. Both parallel and perpendicular sheared flows produce vortex-dominated turbulence.

New analytic theories of magnetic shear induced vortices and other self-organized structures are discussed from the minimization of the appropriate Lagrangian functionals. The minimization is being carried out numerically with the conjugate gradient method. The Lagrangian formulation allows several interpretations: one as a free energy and secondly as pseudo particle motion in a time-dependent potential.

Various dynamical simulations are reviewed. The unstable/stable regimes of the Larichev-Reznik dipoles are discussed. The ∇T_e-monopolar vortices and the magnetic shear induced dipoles are discussed.

Introduction

Initial value simulations of drift wave-Rossby waves and a variety of other plasma wave equations show that once sufficient energy is present in the fluctuations the nonlinearity results in the self-binding or self-organization of the fluctuations into coherent, localized structures. Many examples have been found in the study of drift waves including the effects of magnetic shear,[1] ion-temperature gradients[2, 3, 4, 5] and sheared velocity flows[5, 6, 7, 8] in the equilibrium. Analytical analysis has been used to derive the nonlinear partial differential equation (NLPDE) that govern these stationary structures; however, there are essentially only two highly idealized analytic solutions of the resulting NLPDE. The best known and most useful solution of this class of NLPDE's is the Bessel function double vortex solution given by Larichev and Reznik;[9] the second and third types of solutions are the approximate monopole solutions of Petviashvili[10, 11] and of the type of solution given by the 1D nonlinear oscillation model solution of Su *et al.*[1] Here we develop a numerical method for finding solutions of the equations describing coherent structures.

Coherent Structures Equations

Nonlinear plasma equations of the drift wave type yield a variety of nonlinear equations describing structures moving with a velocity u in the magnetic surface with inhomogeneities of the magnetic field, density, temperature or flow velocities in the x-direction. The general form for the equation governing these structures is

$$\nabla^2\varphi = k^2(u,x)\varphi - \alpha_2(u,x)\varphi^2 - \alpha_3\varphi^3 \tag{1}$$

where the cubic order nonlinearity is positive definite $\alpha_3 > 0$.

Equation (1) is derived in the case of nonlinear drift waves in the presence of an electron temperature gradient[10, 11] η_e and density gradient[12] in which case $\alpha_3 = 0$, $\alpha_2 = \eta_e$ and

$$k^2(u,x) = 1 - \frac{v_d}{u} - \alpha x\ . \tag{2}$$

In the presence of a sheared magnetic field described by the parameter $S_m = L_n/L_s$ the equation[1, 5] is

$$\nabla^2\varphi = \left(1 - \frac{v_d}{u}\right)\varphi - \frac{S_m^2}{u^2}\left(x - \frac{\varphi}{u}\right)\left(x - \frac{\varphi}{2u}\right)\varphi \; . \tag{3}$$

In Eq. (3) we use x, y in units of ρ_s and $\varphi = c\Phi/B(\rho_s v_d) = (e\Phi/T_e)(L_n/\rho_s)$ where $v_d = (cT_e/eBL_N) = \rho_s c_s/L_N$. This equation has nonlinear dipole vortex solutions that are bound together by the cubic $(S_m^2/2u^4)\varphi^3$ restoring force at large φ in the core of the vortex. In the tails of the vortex where $\varphi \ll xu$, Eq. (3) reduces to the linear wave equation

$$\nabla^2\varphi = \left(1 - \frac{v_d}{u} - \frac{S_m^2\, x^2}{u^2}\right)\varphi \tag{4}$$

describing the coupled drift wave-ion acoustic waves in a sheared magnetic field in which $k_{\|}\, L_n = k_y\, \rho_s\, S_m x$.

In fact, the solution of Eq. (1) can be formulated as the stationary point in function space through the variational principle of the Lagrangian $L(\varphi) = \int \mathcal{L}\, dv$ where dv is the relevant volume element and $\mathcal{L}(\varphi, \nabla\varphi, x)$ is the Lagrangian density given below.

Numerical Solutions in 2D

The exact stationary solution $\varphi_s(x, y)$ is a fixed point in functional space of the nonlinear function $N(\varphi)$ defined by Eq. (1). In seeking numerical solutions we seek a sequence of approximations $\varphi^{(k)}$ which converge, in some sense, to $\varphi_s(x, y)$. Since we do not know the exact solution φ_s we cannot form the measure $\|\varphi^{(k)} - \varphi_s\|$. Instead, we seek to measure the convergence through

$$\|N(\varphi)\|^p = \int dv |N(\varphi)|^p \tag{5}$$

where $p = 1, 2, \ldots, \infty$. In finite difference form this measure of error is

$$\|N(\varphi)\|^p = \frac{1}{N_x N_y} \sum_{i,j} |N_{ij}(\varphi)|^p \; . \tag{6}$$

We also introduce the φ-weighted average of $N(\varphi) = 0$ by

$$\langle \varphi, N \rangle = \int dv\, \varphi N(\varphi) = 0 \tag{7}$$

$$= \frac{1}{N_x\, N_y} \sum_{i,j} \varphi_{ij}\, N_{ij}(\varphi) = 0 \; .$$

Using $\varphi\nabla^2\varphi = \nabla\cdot(\varphi\nabla\varphi) - (\nabla\varphi)^2$ we can rewrite the projection $\langle\varphi, N\rangle$ into a sum of energies and the boundary flux F

$$\langle\varphi, N\rangle = \int_V dv \left[(\nabla\varphi)^2 + k^2\varphi^2 - \alpha_2\varphi^3 - \alpha_3\varphi^4\right] - \int_{\partial V} d\ell\, \varphi\, \frac{\partial\varphi}{\partial n} \tag{8}$$

where $\partial\varphi/\partial n$ is also equal to $d\boldsymbol{\ell}\times\hat{\mathbf{z}}\cdot\nabla\varphi$. For a localized structure the boundary term in Eq. (8) is small whereas for a linear structure it is comparable to the two quadratic integrals defined by

$$W^{(2)} = \frac{1}{2}\int dv \left[(\nabla\varphi)^2 + k^2(x,u)\varphi^2\right] \; . \tag{9}$$

Thus, an important feature of the nonlinear structure is the replacement of the boundary term with the nonlinear binding energy in the balance of $\langle\varphi, N\rangle = 0$.

Computing $\langle\varphi, N\rangle$ leads to the nonlinear binding energies

$$W^{(3)} = \alpha_2 \int \varphi^3 dv \tag{10}$$

$$W^{(4)} = \alpha_3 \int \varphi^4 dv \tag{11}$$

that overcome the linear flux $\mathbf{F} = \int_{\partial V} d\ell\, \varphi\, \partial\varphi/\partial n$ in producing the localized state.

Conversion of the Nonlinear Equation into a Sequence of Linear Equations

In seeking a sequence of approximations $\varphi^{(k)}$ that approach a solution of $N(\varphi) = 0$ we use the Newton method in functional space to extrapolate to the solution of $N(\varphi) = 0$. From $\varphi^{(k)}$ we determine $\varphi^{(k+1)}$ by requiring that

$$N\left(\varphi^{(k+1)}\right) \simeq N\left(\varphi^{(k)}\right) + \left.\frac{\delta N}{\delta\varphi}\right|_{\varphi^{(k)}} \left(\varphi^{(k+1)} - \varphi^{(k)}\right) = 0 \tag{12}$$

which gives the linear sequence of equations for $\varphi^{(k+1)}$ requiring the inversion of the inhomogeneous linear operator $(\delta N/\delta\varphi)$ acting on $\varphi^{(k+1)}$. Thus, there are two series of iterations: first, for solving the linear problem for $\varphi^{(k+1)}$ and secondly, the Newton sequence defined by Eq. (12) for $k = 1, 2, 3, \ldots, \infty$.

For the linear problem defined in Eq. (12) of inverting the operator $\widehat{L}(x,y) = (\delta N/\delta\varphi)$ evaluated at $\varphi^{(k)}$ we first tried the methods of successive over-relaxation

(SOR), and related methods. These methods were found to be poorly suited due to the motion of the eigenvalues of $\widehat{L}$ with $\varphi^{(k)}$. We have come to the conclusion that the SOR method is not a suitable method. Subsequently, the search for finding a suitable solution method for inverting $\widehat{L}$ led us to study the ITPACK software of Rice and Boisvert.[13] The conclusion is that algorithms using variations of the conjugate gradient (CG) method are best suited for solving the present problem.

The CG method approach is essentially an algorithm to minimize the quadratic form associated with the linear inversion problem $AX = b$

$$L = \frac{1}{2} X^T AX - X^T b \, .$$

The conjugate gradient method seems to follow the physics of the problem closely and does not require the eigenvalues of A to be less than unity. The convergence and accuracy is poor when the eccentricity of the major-to-minor axes of the hyper ellipsoid $X^T AX$ = const are extreme. The ratio of the maximum major axis to the minimum minor axes is the condition of the matrix.

The standard conjugate gradient method is best suited for matrices that are symmetric and positive definite (SPD). Matrices generated from the finite difference form of Eq. (12) are generally not SPD. Generalizations of the standard conjugate gradient method have been developed to handle non-SPD matrices.[14] A number of these generalized methods are included in the NSPCG (Non-Symmetric Preconditioned Conjugate Gradient) package developed at The University of Texas. The GMRES and ORTHOMIN methods were found to give the best results.

We use both the $p = 1$ one-norm $||N||$ defined in Eq. (6) and the energy constraint $\langle \varphi, N \rangle = 0$ given in Eq. (7) as measures of convergence over the sequence of Newton iterations. The conjugate gradient convergence is a sequence of approximations to minimize the residual $\mathbf{r}$ of the linearized equation (12) so that we do not need to closely monitor the convergence of the CG iterations. In the runs presented here we typically use 50 CG iterations for each Newton iteration.

An example of the convergence trend of $||N||$ versus the number n^{Nt} of Newtonian iterations is shown in Fig. 1. (The convergence example in Fig. 1 is for the structure shown in Fig. 2.) In general there is a rapid decrease of $\|N\|$ for the first 3 or 4 Newton iterations. After that, $\|N\|$ tends to oscillate with a mean value that falls as

$$\|N\| = \frac{\text{const.}}{(n^{Nt})^{5/3}}$$

where n^{Nt} is the number of Newtonian iterations.

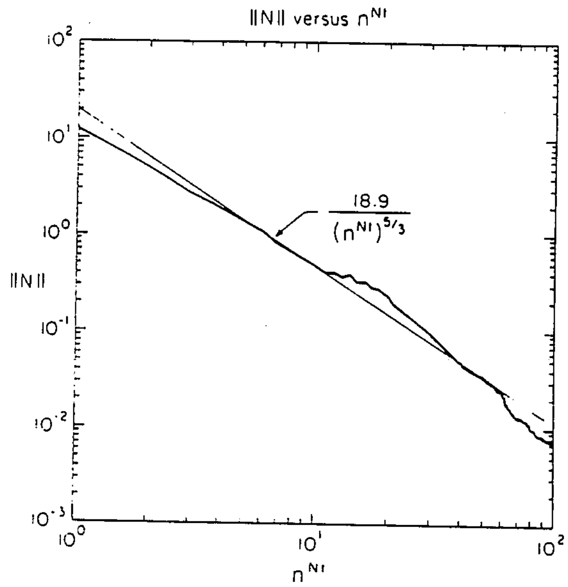

Fig. 1

The energy-like measure of convergence $\langle \varphi, N \rangle$ shows a rapid decrease for the first 3 or 4 Newtonian iterations, then typically oscillates about zero with decreasing swings for 20 to 30 iterations. After this the magnitude of $\langle \varphi, N \rangle$ decreased dramatically. The general trend appears to be for $\langle \varphi, N \rangle$ to finally converge to a small negative number of order a few times $10^{-3}\, W^{n\ell}$ where $W^{n\ell}$ is the nonlinear binding energy. For $n^{Nt} = 60$ the overall decrease in $\|N\|$ is 7×10^{-4} and $\langle \varphi, N \rangle$ is 2×10^{-4} from the initial values as shown in Fig. 1. We believe that the convergence can be continued for considerably larger n^{Nt} values but have not pursued the limiting factors at this time.

Examples of Self-Organized Structures in Inhomogeneous Plasma

Magnetic shear controlled structures

The reduction of the steady-state vortex equations for drift waves in a sheared magnetic field leads to the nonlinear, inhomogeneous pde

$$\nabla^2\psi = \psi - s^2(x-\psi)(x-\psi/2)\psi \tag{13}$$

where the exterior wavenumber $k^2 = 1 - v_d/u$ has been used for the space scale, then the amplitude is rescaled as $\varphi = (u/kv_d)\psi$ and $s^2 = S_m^2\, v_d^2/k^2u^2$ a dimensionless measure of the magnetic shear parameter. The vortex Eq. (13) is invariant under the transformation $\psi \rightarrow -\psi(-x,y)$ giving rise to antisymmetric solutions. In Su *et al.*[1, 12] the nonlinear solutions were investigated with the approximation of slow variation in y compared with x.

With the numerical methods described here we are able to solve the full 2D-nonlinear pde. We find that solutions are qualitatively the same as given in Su *et al.*[1] The prediction of the 1D analysis that $s > s_{\text{crit}}$ is required for a localized self-organized solution is also born out in the 2D solutions. When $s \leq 0.5$ the 2D solutions collapse.

An example of the 2D vortex structure for $s = 1$ is shown in Fig. 2. Figure 2a shows the solution in 2D perspective and Fig. 2b the level contours. The vortex has a dipole vortex core connected to a magnetic shear induced drift-wave ion acoustic wave ($\psi/x < 1$) exterior solution. In terms of the energy components the structure has a linear wave energy of $W^\ell \cong 196$ balanced by a corresponding negative nonlinear binding energy of -196 and a boundary contribution of 0.2. Thus, the self-trapping in 2D is very strong and nearly complete within the $5 \times 5\, k^{-2}$ domain.

In Fig. 3 we compare the profile of the shear induced dipole vortex in Fig. 2 obtained from the slice $\varphi(x, y = 0)$ to the solution obtained using the 1D model (dropping ∂_y^2)

used in Su *et al.*[2]

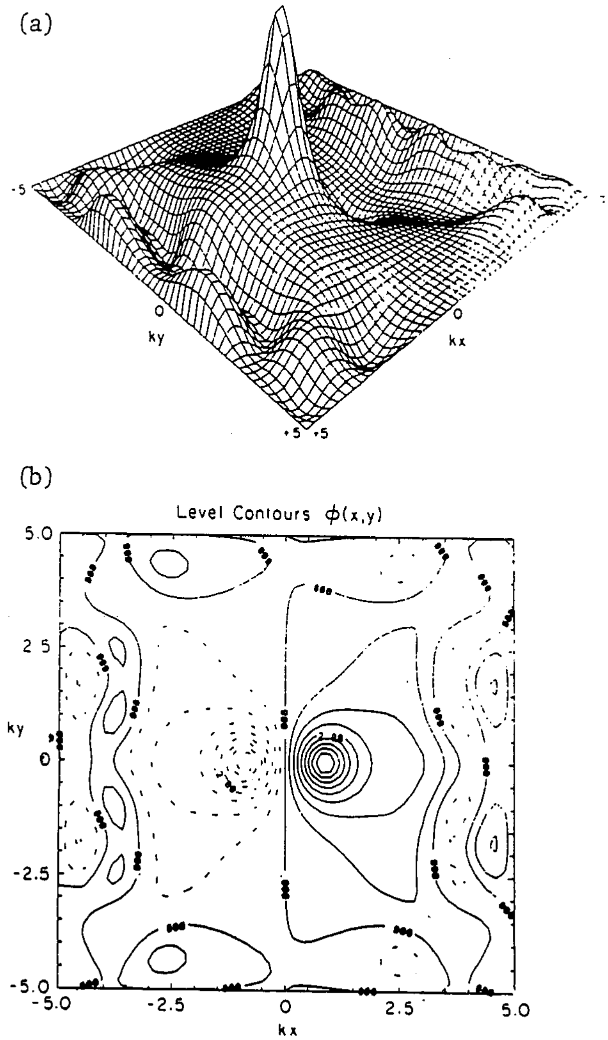

Fig. 2

We see that the 1D model significantly underestimates the strength of the nonlinear binding. While the position of $\varphi_{\max}$ in both cases is nearly the same the $\varphi_{\max}\,(1\text{D}) \simeq 4$ compared with $\varphi_{\max}\,(2\text{D}) = 6.4$.

When the shear parameter is varied we find that the nonlinear structure collapses for $s < s_{\text{crit}} \simeq 0.6$ and that for $s > 1$ the amplitude decreases and the amplitude of exterior wave field increases relative to the amplitude of the vortex core.

For example, for $\varphi_{\max}(s = 1.5) = 4.8$ compared with $(2/3)(6.4) = 4.3$, and for $\varphi_{\max}(s = 2) = 4.0$ compared with $6.4/2 = 3.2$. Thus, the decrease is weaker, closer to $s^{-1/2}$, than the $1/s$ variation estimated in Su *et al.*[1] For the case $s = 2$ the exterior wave field is about one half the amplitude of the vortex core.

Variational Formulation and Conserved Forms

The general equilibrium governed by Eq. (1) can be obtained by varying the following *free energy* functional:

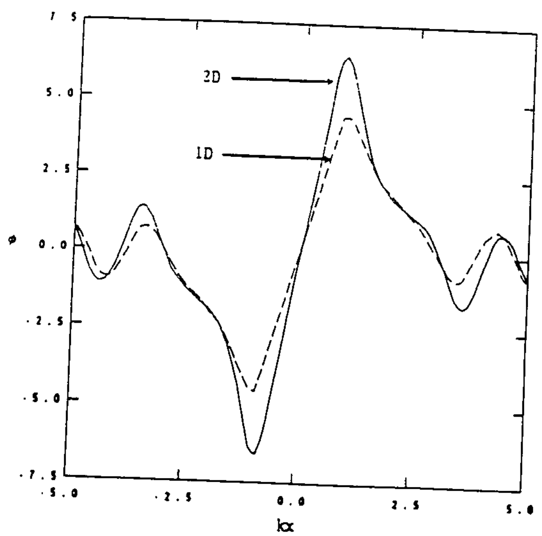

Fig. 3

$$F[\varphi] = \int_V \mathcal{F}(\varphi, \nabla\varphi, \mathbf{x})dv \ , \tag{14}$$

where

$$\mathcal{F}(\varphi, \nabla\varphi, x) = \frac{1}{2}(\nabla\varphi)^2 + \frac{1}{2}k^2\varphi^2 - \frac{1}{3}\alpha_2\varphi^3 - \frac{1}{4}\alpha_3\varphi^4 \ . \qquad (15)$$

Variation of (14) is defined by

$$\delta F[\varphi; \delta\varphi] = \frac{d}{d\varepsilon} F[\varphi + \varepsilon\delta\varphi]\Big|_{\varepsilon=0} = \int_V \frac{\delta F}{\delta\varphi}\,\delta\varphi\, dv \ , \qquad (16)$$

where $\delta\varphi$ is required to vanish on ∂V. Setting the functional derivative $\delta F/\delta\varphi$ to zero we get

$$\frac{\delta F}{\delta\varphi} = -\nabla\cdot\frac{\partial\mathcal{F}}{\partial\nabla\varphi} + \frac{\partial\mathcal{F}}{\partial\varphi} = -\nabla^2\varphi + k^2\varphi - \alpha_2\varphi^2 - \alpha_3\varphi^3 = 0 \ , \qquad (17)$$

which is Eq. (1).

One can interpret this free energy functional variational principle for the equilibrium as an action principle, alá Hamilton's principle of mechanics, for various pseudo dynamics. For example, in the case where restriction to a single spatial dimension, say x, is made, the equilibrium becomes equivalent to a one and a half degree-of-freedom Hamiltonian system. Here the role of time is played by x and the role of the coordinate is played by φ. The free energy density $\mathcal{F}$ can then be interpreted as a Lagrangian L, where

$$L \equiv \frac{1}{2}\varphi_x^2 - V_{\text{eff}}(\varphi, x) \qquad (18)$$

with

$$V_{\text{eff}}(\varphi, x) \equiv -\frac{1}{2}k^2\varphi^2 + \frac{1}{3}\alpha_2(x)\varphi^3 + \frac{1}{4}\alpha_3(x)\varphi^4 \ . \qquad (19)$$

Observe that the vanishing of $\delta\varphi$ on the boundary is the appropriate end condition for Hamilton's principle. In the case where α_2 is "time" independent and $\alpha_3 = 0$, (19) becomes the potential for ion-acoustic solitons.

The case for Eq. (13), where α_2 and k^2 vary with x, is considered in detail in Su *et al.*[1] and the phase space dynamics is shown here in Fig. 4. The Hamiltonian in this case is given by Legendre transform as follows:

$$H = p\varphi_x - \mathcal{L} = \frac{p^2}{2} + V_{\text{eff}}(\varphi, x) \qquad (20)$$

where $p = \frac{\partial L}{\partial\varphi_x} = \varphi_x$. Constant energy levels at a sequence of $t = kx$ values are shown in Fig. 4.

In Fig. 4 the effective time variable is $t = kx$, the coordinate q is the potential ψ and the momentum p the electric field $d\psi/dt$. The dipole solution given in Fig. 3 corresponds to throwing the effective ball down from $\psi = 0$ with various values of velocity into the time-dependent potential. The result is that there is a whole spectrum of nonlinear solutions with various values of $d\psi/dt$, or internal electric field, for which there are localized, self-organized plasma structures.

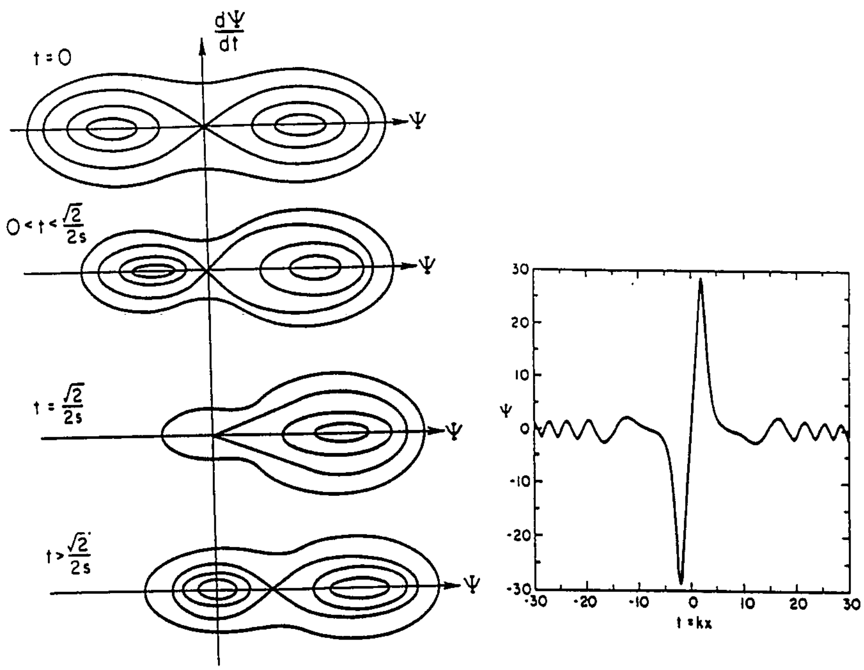

Fig. 4

The creation of these self-organized structures is a method the plasma has of storing, in a small concentrated region, considerable energy. It is perhaps natural that the unstable or out of equilibrium plasma would choose to put part of its free energy into these efficient capacitor-like storage banks.

Acknowledgments

This work was supported by the U.S. Department of Energy contract #DE-FG05-80ET-53088.

References

[1]X-N. Su, W. Horton, and P.J. Morrison, Phys. Fluids B 4, 1238 (1992).

[2]S. Hamaguchi and W. Horton, Phys. Fluids B **2**, 1833 (1990).

[3]M. Ottaviani, F. Romanelli, R. Benzi, M. Briscolini, P. Santangelo, S. Succi, Phys. Fluids B **2**, 67 (1990).

[4]B.G. Hong, F. Romanelli, and M. Ottaviani, Phys. Fluids B **3**, 615 (1991).

[5]W. Horton, D. Jovanović, and J. Juul Rasmussen, "Vortices Associated with Toroidal Ion Temperature Gradient Driven Fluctuations," to appear in Phys. Fluids B, October 1992.

[6]W. Horton, T. Tajima, and T. Kamimura, Phys. Fluids **30**, 3485 (1987).

[7]T. Tajima, W. Horton, P.J. Morrison, J. Schutkeker, T. Kamimura, K. Mima, and Y. Abe, Phys. Fluids B **3**, 938 (1991).

[8]S. Hamaguchi and W. Horton, Phys. Fluids B **4**, 319 (1992).

[9]V.D. Larichev and G.M. Reznik, Oceanology **16**, 547 (1976).

[10]V.I. Petviashvili, Fiz. Plasmy **3**, 270 (1977) [Sov. J. Plasma Phys. **3**, 150 (1977)].

[11]K.H. Spatschek, E.W. Laedlke, Chr. Marquardt, S. Musher, H. Wenk, Phys. Rev. Lett. **64**, 3027 (1990).

[12]X.N. Su, W. Horton and P.J. Morrison, Phys. Fluids B **3**, 921 (1991).

[13]J. Rice and R. Boisvert, Solving Elliptic Problems Using ELLPACK, New York, Springer-Verlag, 1985.

[14]T.C. Oppe, W.D. Joubert, and D.R. Kincaid, NSPCG User's Guide Version 1.0, CNA-216, April, 1988, and ITPACK 2D User's Guide, D.R. Kincaid, T.C. Oppe, D.M. Young, CNA-232 (1989).